European Radiology (2019) 29:5950–5960
https://doi.org/10.1007/s00330-019-06217-5

COMPUTED TOMOGRAPHY

# Sparse sampling computed tomography (SpSCT) for detection of pulmonary embolism: a feasibility study

Andreas P. Sauter[1] · Felix K. Kopp[1] · Rolf Bippus[2] · Julia Dangelmaier[1] · Dominik Deniffel[1] · Alexander A. Fingerle[1] · Felix Meurer[1] · Daniela Pfeiffer[1] · Roland Proksa[2] · Ernst J. Rummeny[1] · Peter B. Noël[1]

Received: 3 December 2018 / Revised: 1 March 2019 / Accepted: 2 April 2019 / Published online: 9 May 2019


## Abstract

**Objectives** Evaluation of sparse sampling computed tomography (SpSCT) regarding subjective and objective image criteria for the detection of pulmonary embolism (PE) at different simulated dose levels.

**Methods** Computed tomography pulmonary angiography (CTPA) scans of 20 clinical patients were used to obtain simulated low-dose scans with 100%–50%–25%–12.5%–6.3%–3.1% of the clinical dose, resulting in a total of six dose levels (DL). From these full sampling (FS) data, every second (2-SpSCT) or fourth (4-SpSCT) projection was used to obtain simulated sparse sampling scans. Each image set was evaluated by four blinded radiologists regarding subjective image criteria (artifacts, image quality) and diagnostic performance (confidence, sensitivity, specificity, accuracy, and area under the curve). Additionally, the contrast-to-noise ratio (CNR) was evaluated for objective image quality.

**Results** Sensitivity was 100% with 2-SpSCT and 4-SpSCT at the 25% DL and the 12.5% DL for all localizations of PE (one subgroup 98.5%). With FS, the sensitivity decreased to 90% at the 12.5% DL. 2-SpSCT and 4-SpSCT showed higher values for sensitivity, specificity, accuracy, and the area under the curve at all DL compared with FS. Subjective image quality was significantly higher for 4-SpSCT compared with FS at each dose level ($p < 0.01$, paired $t$ test). Only with 4-SpSCT, all examinations were rated as showing diagnostic image quality at the 12.5% DL.

**Conclusions** Via SpSCT, a dose reduction down to a 12.5% dose level (corresponding to a mean effective dose of 0.38 mSv in the current study) for CTPA is possible while maintaining high image quality and full diagnostic confidence.

**Key Points**

- *With sparse sampling CT, radiation dose could be significantly reduced in clinical routine.*
- *Sparse sampling CT is a novel hardware solution with which less projection images are acquired.*
- *In the current study, a dose reduction of 87.5% (corresponding to a mean effective dose of 0.38 mSv) for CTPA could be achieved while maintaining excellent diagnostic performance.*

**Keywords** Pulmonary embolism · Computed tomography angiography · Radiation dosage · Technology, radiologic · Patient safety

Andreas P. Sauter and Felix K. Kopp contributed equally to this work.

✉ Andreas P. Sauter
andreas.sauter@tum.de

[1] Department of Diagnostic and Interventional Radiology, Technical University of Munich, Munich, Germany

[2] Philips GmbH Innovative Technologies, Research Laboratories, Hamburg, Germany

**Abbreviations**

| | |
|---|---|
| ALARA | As low as reasonably achievable |
| AUC | Area under the receiver operating characteristic curve |
| BMI | Body mass index |
| CNR | Contrast-to-noise ratio |
| CT | Computed tomography |
| $CTDI_{VOL}$ | Volume-weighted CT dose index |
| CTPA | CT pulmonary angiography |
| DL | Dose level |
| DLP | Dose length product |

| | |
|---|---|
| ED | Effective dose |
| FS | Full sampling |
| HU | Hounsfield units |
| IQ | Image quality |
| PE | Pulmonary embolism |
| ROC | Receiver operating curve |
| ROI | Region of interest |
| SD | Standard deviation |
| SpSCT | Sparse sampling CT |

## Introduction

Pulmonary embolism (PE) is a common disease with a possible lethal outcome [1]. For diagnosis or rule-out of PE, CT pulmonary angiography (CTPA) is seen as the gold standard under routine clinical conditions [2]. CTPA, available around the clock in most hospitals, can be performed quickly and is relatively cost-efficient. With CTPA, higher resolution, shorter examination times, and higher sensitivities and specificities can be obtained compared with other techniques like ventilation-perfusion scintigraphy [3]. However, CTPA involves a high radiation exposure with reported average effective doses (ED) of 2.7–4.5 mSv nowadays [4, 5]. Radiation exposure is a concern due to the ionization of DNA and thus of the possible increased lifetime risk for malignancy, especially when applied to young patients [6]. In consequence, it is essential to develop dose reduction strategies for computed tomography (CT) examinations. However, image quality must be suitable, according to the principle of "as low as reasonably achievable" (ALARA).

There are numerous established techniques for dose reduction [7–9]. Over the last decade, iterative reconstruction algorithms made improved image quality and/or reduction of radiation exposure possible [10]. Via novel model-based iterative reconstruction algorithms, additional reduction of radiation exposure was realized, even compared with first-generation hybrid iterative algorithms [11, 12]. With these iterative algorithms, an ED in the range of 1.1–2.29 mSv can be achieved for CTPA [4, 13, 14]. However, dose reduction is limited as noise increases with decreased tube currents which only can partially be compensated by iterative reconstruction algorithms.

Further reduction of radiation exposure could be achieved by novel CT concepts such as sparse sampling CT (SpSCT) [15, 16]. With this technique, fewer projection images are acquired (e.g., only every second or fourth projection is obtained). Compared with conventional CT systems, the radiation exposure of every projection can be increased, but the total radiation dose is reduced as fewer projections are obtained. As individual projections are obtained with a higher tube current, overall noise can be further reduced compared with conventional CT systems. This especially accounts for low-dose CT examinations. At the same time however, the angular sampling decreases and regardless of the reconstruction algorithm image quality will eventually degrade because insufficient data becomes notable as streak artifacts. For a moderate decrease in angular sampling, this can be compensated by fully iterative reconstruction obtaining a trade-off between streak and noise-induced artifacts. Until now, no sparse sampling capable hardware (e.g., novel x-ray tubes) is available for patient examinations. However, development efforts over the last years have shown that the development of such equipment is making progress and that implementation into clinical routine could become feasible [17]. Wiedmann et al provided a technical overview of approaches to implement x-ray pulsing for CT [18]. They also show the feasibility of fast pulsing x-ray tubes with a research prototype. As the current work focusses on the clinical evaluation of sparse sampling simulations, we would like to refer interested reader to the before mentioned work for technical details on the hardware realization of sparse sampling. First studies on simulated SpSCT illustrated promising results, e.g., regarding dose reduction [19–22].

In the present study, simulated SpSCT was compared with conventional CT at different simulated dose levels based on clinical scans of patients with suspected PE. The aim was to examine the feasibility of using SpSCT regarding subjective and objective performance with respect to image quality, diagnostic confidence, and diagnostic performance.

## Material and methods

### Patient population

Twenty patients with suspected PE were included in this study. Ten patients (50%) were diagnosed positive and negative for PE, respectively. PE was classified as central, segmental, or subsegmental. PE in multiple locations was also possible. Central PE was defined as an embolus in the pulmonary trunk or in the right/left main pulmonary artery (including saddle embolus at the bifurcation of the interlobar and the upper lobar artery on the right side and of the upper and lower lobar artery on the left side). Segmental pulmonary embolism was defined as a pulmonary embolism in the lobar arteries and the segmental arteries (including saddle embolus at the bifurcation of subsegmental arteries). Subsegmental pulmonary embolism was defined as an embolus in the subsegmental arteries. Central PE was present in six cases and each segmental and subsegmental PE was present in ten cases. Thus, all patients with central PE also showed segmental and subsegmental PE and all patients with segmental PE also showed subsegmental PE. No patients with subsegmental PE alone were present. No preselection regarding patient weight, age, sex, or other characteristics was performed. All data were anonymized for all study purposes.

## CTPA image acquisition

All patients were examined using a state-of-the-art CT system (Brilliance iCT; Philips Healthcare), with a standard CTPA protocol. The scan range included the whole lung and was specified by an anteroposterior scout. The scan was started using a bolus tracker in the pulmonary trunk (threshold, 100 HU). The scan was performed craniocaudally with a pitch of 0.9, a 128 × 0.625-mm detector configuration, and a 512 × 512 image matrix. Tube voltage was determined by the patient's weight with voltages of 120 kVp (BMI ≥ 25 kg/m$^2$) or 100 kVp (BMI < 25 kg/m$^2$). Tube current was automatically adjusted by the system, including *z*-axis modulation. For every patient, the automatically generated dose protocol was extracted after the examination. Tube voltage (kVp), tube current (mA), volume-weighted CT dose index ($CTDI_{vol}$), and dose length product (DLP) were collected. By multiplication of DLP by the chest conversion factor (0.0145), the effective dose (ED) could be calculated [23]. Mean ED for all patients was 3.03 mSv. ED was 3.41 mSv for patients positive for PE and 2.64 mSv for patients negative for PE.

## Simulation and reconstruction of low-dose and sparse sampling images

Lower dose data was obtained using a low-dose simulation tool [24, 25]. Simulation includes producing projection data with noise properties realistically close to the projection data up to the third statistical moment as would be obtained by a real scan at lower tube currents. This method was shown to produce realistic simulations of low-dose data for the scanner type used in the current study [20]. CTPA raw data were used to simulate CTPA scans with reduced tube currents, resulting in dose levels (DL) of 50%, 25%, 12.5%, 6.3%, and 3.1% of the original dose. All other scan parameters remained identical yielding 6 datasets per patient at full sampling (FS) with 2400 views per turn.

To obtain sparse angular sampling, projection data were further processed by extracting every second projection view (2-SpSCT with 1200 views per turn) or every fourth projection view (4-SpSCT with 600 views per turn). Beyond every fourth projection, we observed that the angular sampling becomes insufficient to reconstruct descent images at the desired image resolution without major artifacts (Table 1). The combination of low-tube current simulation and angular sparsity yielded another five 2-SpSCT datasets at 50 to 3.1% DL and another four 4-SpSCT datasets at 25 to 3.1% DL. 2-SpSCT at 100% dose and 4-SpSCT at 100% and 50% dose could not be obtained as all images were simulated based on FS images at 100% dose. Thus, the radiation dose per view would be higher than the original dose with 2-SpCT and 4-SpSCT at the named dose levels which cannot be simulated.

**Table 1** Percentage of cases without artifacts ± SD between readers. With SpSCT, more cases without artifact were present at lower dose levels. At the 6.3% dose level, 45% of all cases showed no artifact with FS whereas 71% of all cases showed no artifacts with 4-SpSCT

| Cases without artifacts | | | |
|---|---|---|---|
| Dose level | Full sampling | 2-SpSCT | 4-SpSCT |
| 100% | 78 ± 24% | \ | \ |
| 50% | 84 ± 18% | 78 ± 21% | \ |
| 25% | 74 ± 20% | 75 ± 23% | 68 ± 39% |
| 12.5% | 69 ± 11% | 75 ± 19% | 78 ± 25% |
| 6.3% | 45 ± 20% | 70 ± 18% | 71 ± 25% |
| 3.1% | 26 ± 19% | 45 ± 17% | 60 ± 33% |

Images were reconstructed using fully iterative, model-based MLIR reconstruction to remove artifacts (mainly streaks) introduced by sparse sampling [26] using a Huber penalty term. The reconstruction algorithm used a fully automatic procedure to control the regularization parameter (weight of the roughness penalty [26]). It uses a SNR measure defined as the mean standard deviation (SD) within small local neighborhoods (125) of voxels that were identified as lying in a homogeneous (edge free) region of the image prior to reconstruction, based on an edge detection and segmentation of the smoothed FBP-reconstructed start image [27, 28]. The algorithm is described in detail in [29]. A noise level with 9 HU SD was chosen to obtain a comparable "look and feel" in terms of image properties introduced by edge-preserving regularization, commonly referred to as "patchiness" for all images and to refrain from manually tuning to optimal CNR or other image properties, possibly introducing an undesirable bias into the evaluation.

The total of 300 datasets was processed and reconstructed on a 0.75-mm axial grid with 0.7 mm slice thickness using the identical algorithm and parameter settings.

## Contrast-to-noise ratio

For objective evaluation of image quality, the contrast-to-noise ratio (CNR) with respect to homogeneous regions in the muscle was obtained for central vessels ($CNR_{CENTRAL}$) and peripheral vessels ($CNR_{PERIPHERAL}$). For $CNR_{CENTRAL}$, three circular ROIs were placed in the pulmonary trunk, the right main pulmonary artery, and the left main pulmonary artery. For $CNR_{PERIPHERAL}$, four circular ROIs were placed in segmental arteries of the right and the left lung. For each vessel, the respective intensity values were measured (Hounsfield units, HU). Two ROIs were placed in the right and the left paraspinal muscle and the arithmetic mean of both ROIs was calculated ($S_m$). For each vessel, CNR was calculated by the following: $\frac{S_V - S_M}{noise}$, where $S_V$ is the intensity

measured in the vessel, $S_M$ is the intensity of paravertebral muscle, and noise is given as the SD measured in the muscle.

### Subjective image quality

Each dataset was independently evaluated by four radiologists (board certified, 4.3 ± 1.3 years of experience). Readers were blinded to the diagnosis and reconstruction parameters (dose level and level of sparse sampling). Image parameters (slice thickness, window level, and width) should not be changed by the readers for the evaluation of subjective image quality and artifacts. Subjective image quality should be rated as an overall image impression with focus on the pulmonary vessels and the recognizability of possible pulmonary embolism. Subjective image quality was rated regarding the following criteria: 1—not diagnostic; 2—sufficient; 3—satisfactory; 4—good; 5—very good; 6—excellent. The presence of artifacts was assessed using the classes: no artifacts, streaking artifacts, ring artifacts, other artifacts.

### Diagnostic confidence regarding detection of PE

Image parameters (slice thickness, window level, and width) could be individually chosen by the readers for diagnosis of PE. Diagnostic confidence regarding detection of PE was rated for each localization (central, segmental, subsegmental) separately. Hereby, confidence was classified in six levels: 1—no PE, completely confident; 2—no PE, probably confident; 3—no PE, poor confidence, additional imaging needed; 4—PE present, poor confidence, additional imaging needed; 5—PE present, probably confident; 6—PE present, completely confident. Ratings of 1, 2, and 3 were considered negative for PE and ratings of 4, 5, and 6 as positive for PE.

If subjective image quality (cf. respective section) was rated as 1 (not diagnostic), diagnostic confidence was defined as 3 (no PE, poor confidence, additional imaging needed) as a PE could not be clearly diagnosed due to image quality. PE should only be rated as positive in the specific location when a clear embolus was visible.

### Statistical analysis

Statistical analysis was performed by dedicated software packages (SPSS, IBM; Excel 2016, Microsoft; Prism 7). Continuous data are expressed as arithmetic mean ± SD. Data were tested for Gaussian distribution via D'Agostino-Pearson omnibus test. As Gaussian distribution was present, a paired *t* test was used for evaluation of CNR and subjective image quality when comparing two groups, respectively. When comparing three groups (FS, 2-SpSCT, and 4-SpSCT), repeated measures ANOVA with Bonferroni correction was used. A $p$ value $\leq 0.05$ was considered to indicate statistical significance for *t* tests and ANOVA tests. Subjective image quality is shown in box-and-whisker plots, including mean, median, 25/75% quartile, whiskers (10th–90th percentile), and outliers. Interreader agreement was tested by Fleiss' kappa ($\kappa$). Hereby, values < 0 are indicating no agreement. A value of 0–0.20 is indicating slight, 0.21–0.40 fair, 0.41–0.60 moderate, 0.61–0.80 substantial, and 0.81–1 almost perfect agreement [30].

Each case was defined as positive ($PE_P$) or negative ($PE_N$) for central, segmental, and subsegmental PE based on a consensus reading of two experienced radiologists using full-dose images (clinical standard); this consensus was defined as ground truth.

If a reader evaluated the case as negative for PE but there was a PE present, this was regarded as false negative ($f_N$). If a reader stated that the diagnosis was not possible due to image quality in a case with a PE present, this was rated as false negative due to image quality ($f_{NIQ}$). Sensitivity was calculated using the following equation:

$$\text{Sensitivity} = \left(1 - \frac{\sum f_N + \sum f_{NIQ}}{\sum PE_P}\right) \cdot 100\%$$

If a reader evaluated the case as positive for PE but there was no PE present, this was regarded as false positive ($f_P$). If a reader stated that the diagnosis was not possible due to image quality and there was no PE present, this was rated as false positive due to image quality ($f_{PIQ}$). Specificity is given by:

$$\text{Specificity} = \left(1 - \frac{\sum f_P + \sum f_{PIQ}}{\sum PE_N}\right) \cdot 100\%$$

The overall accuracy is the percentage of right classifications over all cases:

$$\text{Accuracy} = \left(1 - \frac{\sum f_N + \sum f_{NIQ} + \sum f_P + \sum f_{PIQ}}{\sum PE_P + \sum PE_N}\right) \cdot 100\%$$

Sensitivity, specificity, and accuracy were computed for each reader separately. Results are given as arithmetic mean ± SD.

The area under the receiver operating characteristic curve (AUC) was computed with the empirical ROC curve. The AUC represents the probability that a randomly chosen diseased subject is ranked with greater suspicion than a randomly selected healthy subject [31].

## Results

### Contrast-to-noise ratio

$CNR_{CENTRAL}$ and $CNR_{PERIPHERAL}$ were higher at higher dose levels and decreased at lower dose levels (Fig. 1). A significant difference between sampling types was found between

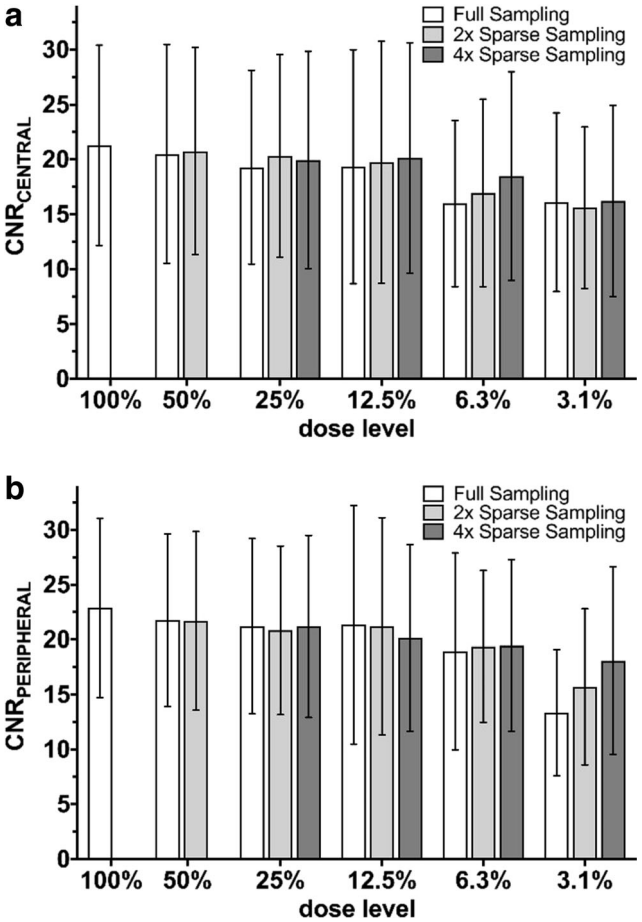


**Fig. 1** (**a**) $CNR_{CENTRAL}$ and (**b**) $CNR_{PERIPHERAL}$ for the different dose levels and localizations of PE. A significant difference was found between 4-SpSCT and FS at the 3.1% dose level for $CNR_{PERIPHERAL}$

FS and 4-SpSCT at the 3.1% DL for $CNR_{PERIPHERAL}$ ($p < 0.01$). Repeated measures ANOVA did not show a significant difference between the three groups.

### Subjective image quality

A comparison of images simulated with FS, 2-SpSCT, and 4-SpSCT at the different dose levels is shown in Fig. 2. An enlarged view of FS and 4-SpSCT at the 12.5% DL is shown in Fig. 3. Repeated measures ANOVA to test for differences between the three groups (FS, 2-SpSCT, and 4-SpSCT) showed a significant difference ($p < 0.001$). Bonferroni-adjusted post hoc analysis revealed a significant difference between FS and 2-SpSCT ($p = 0.0045$) as well as between FS and 4-SpSCT ($p = 0.001$); the difference between 2-SpSCT and 4-SpSCT did not show statistical significance ($p = 0.38$).

Mean subjective image quality was higher with 2- and 4-SpSCT compared with FS as well as with 4-SpSCT compared with 2-SpSCT at each DL. IQ was rated as higher than 4 (good image quality) with 2- and 4-SpSCT at the 25% DL. IQ was rated as higher than 3 (satisfactory image quality) at the 12.5% and the 6.3% DL for 4-SpSCT as well as at the 12.5% DL for 2-SpSCT. Significant differences (paired $t$ test) were found between 4-SpSCT and FS at each DL ($p = 0.023$ or lower), between 2-SpSCT and FS at each DL aside from the 12.5% DL ($p = 0.017$ or lower), and between 4-SpSCT and 2-SpSCT at the 12.5% DL ($p = 0.0047$) as shown in Fig. 4.

### Detection of PE

Mean sensitivity was greater than 95% for all sampling schemes down to the 25% DL. A further dose reduction to 12.5% led to a decreased sensitivity of approximately 90% for FS. With SpSCT, readers still reached a sensitivity of exactly 100% (except 4-SpSCT for segmental PE with a sensitivity of 97.5%) at this DL. The sensitivity decreased with further dose reduction for all sampling schemes, with higher sensitivities for SpSCT. Results for specificity showed a similar trend as for sensitivity (Table 2).

High accuracies were obtained with FS down to the 25% DL and down to the 12.5% DL with 2- and 4-SpSCT, respectively. At the 3.1% DL, accuracy with FS was below 50%, with 2-SpSCT around 70%, and with 4-SpSCT around 75% (Table 2).

Excellent AUC was obtained down to the 12.5% DL with FS, down to the 6.25% DL with 2-SpSCT, and down to the 3.1% DL with 4-SpSCT.

Interreader agreement (Fleiss $\kappa$) was higher for 2-SpSCT and 4-SpSCT compared with FS at all dose levels and sections of PE. At the 25% and the 12.5% dose levels, similar $\kappa$-values for 2-SpSCT and 4-SpSCT resulted. At the lowest dose levels (6.3% and 3.1%), there was a tendency to higher $\kappa$-values for 4-SpSCT. Substantial agreement regarding central and segmental PE could be shown for 2-SpSCT and 4-SpSCT down to the 12.5% dose level.

### Diagnostic confidence of readers

High diagnostic confidences were found at high dose levels (100%, 50%, and 25%) for all localizations and sampling schemes. At lower dose levels, a higher percentage of all cases showed a high confidence with SpSCT compared with FS (Table 3). Figure 5 shows the rating for the 12.5% DL.

## Discussion

In the present study, the possibility of dose reduction in CTPA scans by using sparse sampling as a novel CT technology was evaluated.

Previous studies showed that a further dose reduction via (iterative) reconstruction algorithms or other software solutions is limited [14, 32]. A further considerable reduction in

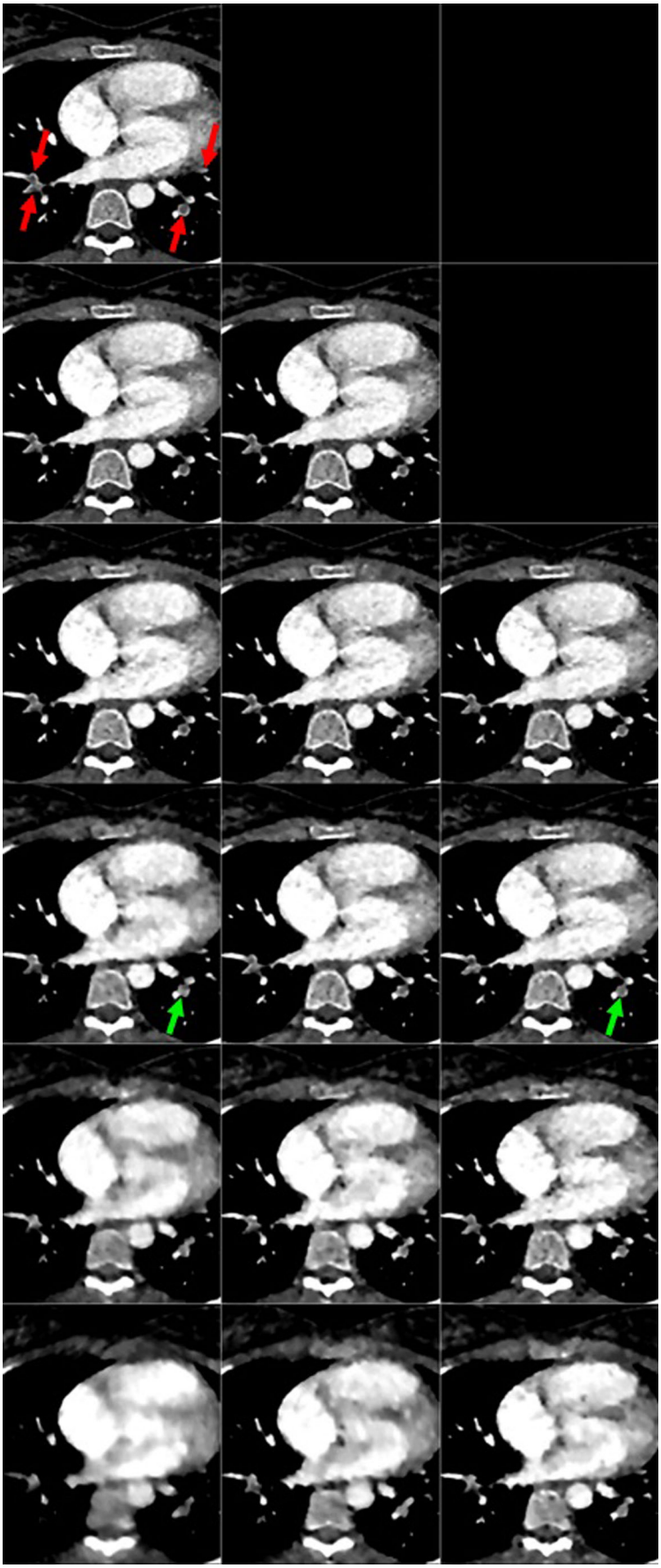

◀**Fig. 2** Shown are FS (left column), 2-SpSCT (middle column), and 4-SpSCT (right column) images at the different dose levels (from top to bottom: 100%–50%–25%–12.5%–6.3%–3.1%). Shown is a case with pulmonary embolisms in segmental arteries of both lower lobes (red arrows). Image quality clearly decreases at lower dose levels with higher quality at 4-SpSCT images. E.g., the embolus in the left segmental artery can be clearly visualized with 4-SpSCT at 12.5% dose, whereas a detection with FS at the same dose is less distinctive (green arrows).

radiation dose seems only feasible with new hardware solutions like photon-counting CT or sparse sampling CT [33]. To the authors' knowledge, the present study is the first to systematically evaluate the diagnostic performance of sparse sampling simulations based on clinical CTPA scans. In theory, radiation dose can be reduced by using sparse sampling, especially at already low dose levels because the relative contribution of noise to the measurements increases with lower tube currents. With sparse sampling, every projection can be obtained with a higher tube current and thus, less noise is present in each single projection.

As expected, high sensitivities could be found with FS at higher dose levels (100%, 50%, and 25%) with sensitivities of 95% or more for all localizations of PE. This result corresponds to other studies showing high sensitivities for images with reduced dose when using iterative reconstruction [12]. In the current study, a novel fully iterative reconstruction algorithm was used (MLIR) [10]. Given the results of high sensitivities with FS down to the 25% dose level, a dose reduction with MLIR alone seems possible. However, sensitivities were higher with SpSCT compared with FS at all comparable dose levels. Hereby, sensitivities of 100% could be shown with 2-SpSCT and with 4-SpSCT at the 25% and the 12.5% DL for all localizations of PE (except 4-SpSCT at the 12.5% DL for segmental PE). We observed sensitivities of less than 100%

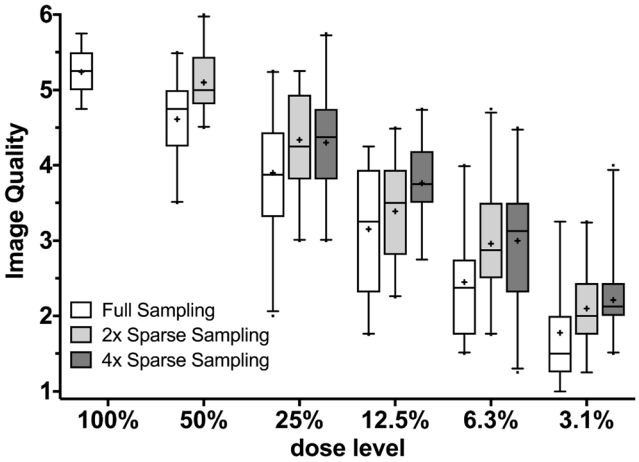


**Fig. 4** Box-and-whiskers plots of the subjective image quality (6 = excellent; 1 = not diagnostic). IQ was rated better with SpSCT than with FS and better with 4-SpSCT than with 2-SpSCT at each dose level. Differences between 4-SpSCT and FS were significant at each dose level. Between 4-SpSCT and 2-SpSCT, a significant difference was found at the 12.5% dose level. Between 2-SpSCT and FS, a significant difference was found at all dose levels apart from the 12.5% dose level

even at full-dose images. In the context of this study, a sensitivity of 100% seems not always achievable even by an experienced radiologist as each reader had to determine if a PE was present or absent in each localization. In consequence, an incorrect diagnosis rating is not necessarily wrong in a clinical setup, e.g., a PE could be determined as central and segmental but was only diagnosed as segmental by the reader.

Mean subjective IQ was significantly higher with 4-SpSCT compared with FS at all dose levels. IQ was rated as better than 4 at the 25% DL and better than 3 at the 12.5% DL for 2- and 4-SpSCT. With 4-SpSCT, mean IQ was 3.8 at the 12.5% DL and thus significantly better than with 2-SpSCT. The number of non-diagnostic examinations could be lowered from 1.5

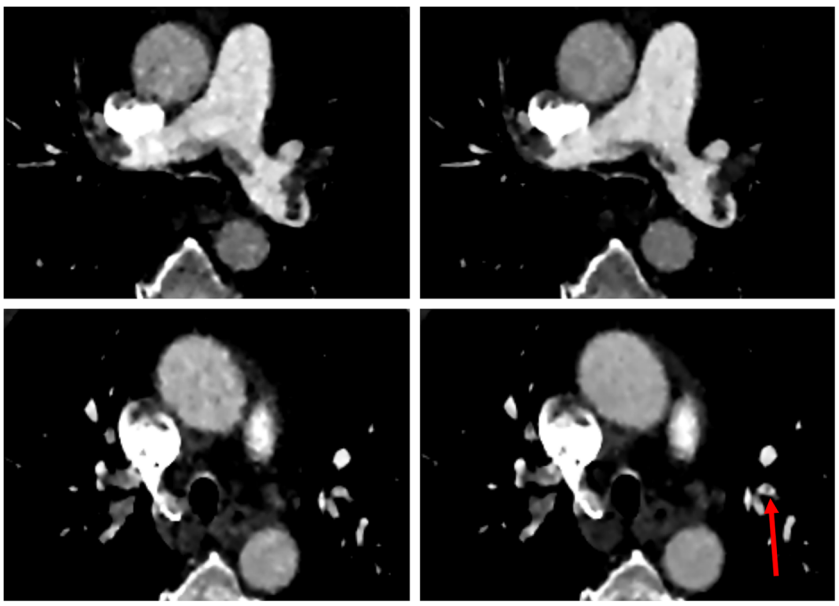

**Fig. 3** Comparison of FS (left) and 4-SpSCT (right) at the 12.5% dose level. Shown are the central (top) and peripheral (bottom) pulmonary arteries with a central saddle embolus and multiple emboli in the segmental and subsegmental arteries, respectively. Overall, image quality with 4-SpSCT is higher and small emboli (red arrow) can only visualized in this dataset

**Table 2** Sensitivity, specificity, accuracy, the area under the curve (AUC), and interreader agreement at the different localizations of PE for all sampling schemes and dose levels

| | | | | | | | | | |
|---|---|---|---|---|---|---|---|---|---|
| Sensitivity | | | | | | | | | |
| | Full sampling | | | 2-SpSCT | | | 4-SpSCT | | |
| Dose level | Central | seg. | sub-seg. | Central | seg. | sub-seg. | Central | seg. | sub-seg. |
| 100% | 96 ± 8% | 98 ± 5% | 98 ± 5% | \ | \ | \ | \ | \ | \ |
| 50% | 96 ± 8% | 100 ± 0% | 100 ± 0% | 96 ± 8% | 95 ± 10% | 95 ± 10% | \ | \ | \ |
| 25% | 96 ± 8% | 98 ± 5% | 98 ± 5% | 100 ± 0% | 100 ± 0% | 100 ± 0% | 100 ± 0% | 100 ± 0% | 100 ± 0% |
| 12.50% | 92 ± 17% | 90 ± 14% | 90 ± 14% | 100 ± 0% | 100 ± 0% | 100 ± 0% | 100 ± 0% | 98 ± 5% | 100 ± 0% |
| 6.30% | 71 ± 28% | 78 ± 22% | 78 ± 22% | 96 ± 8% | 90 ± 8% | 93 ± 10% | 92 ± 10% | 93 ± 10% | 98 ± 5% |
| 3.10% | 25 ± 10% | 40 ± 14% | 40 ± 14% | 58 ± 17% | 80 ± 14% | 78 ± 13% | 92 ± 17% | 85 ± 10% | 85 ± 10% |
| Specificity | | | | | | | | | |
| | Full sampling | | | 2-SpSCT | | | 4-SpSCT | | |
| Dose level | Central | seg. | sub-seg. | Central | seg. | sub-seg. | Central | seg. | sub-seg. |
| 100% | 96 ± 4% | 100 ± 0% | 100 ± 0% | \ | \ | \ | \ | \ | \ |
| 50% | 98 ± 4% | 100 ± 0% | 100 ± 0% | 100 ± 0% | 100 ± 0% | 100 ± 0% | \ | \ | \ |
| 25% | 95 ± 7% | 95 ± 6% | 95 ± 6% | 96 ± 7% | 98 ± 5% | 98 ± 5% | 95 ± 7% | 98 ± 5% | 95 ± 10% |
| 12.50% | 91 ± 4% | 90 ± 14% | 88 ± 15% | 95 ± 4% | 95 ± 6% | 95 ± 6% | 96 ± 4% | 100 ± 0% | 98 ± 5% |
| 6.30% | 82 ± 9% | 85 ± 17% | 78 ± 19% | 93 ± 8% | 95 ± 6% | 95 ± 6% | 88 ± 12% | 85 ± 17% | 85 ± 17% |
| 3.10% | 48 ± 18% | 48 ± 30% | 45 ± 31% | 71 ± 24% | 68 ± 33% | 60 ± 32% | 75 ± 32% | 68 ± 47% | 65 ± 45% |
| Accuracy | | | | | | | | | |
| | Full sampling | | | 2-SpSCT | | | 4-SpSCT | | |
| Dose level | Central | seg. | sub-seg. | Central | seg. | sub-seg. | Central | seg. | sub-seg. |
| 100% | 96 ± 3% | 99 ± 3% | 99 ± 3% | \ | \ | \ | \ | \ | \ |
| 50% | 98 ± 5% | 100 ± 0% | 100 ± 0% | 99 ± 3% | 98 ± 5% | 98 ± 5% | \ | \ | \ |
| 25% | 95 ± 4% | 96 ± 5% | 96 ± 5% | 98 ± 5% | 99 ± 3% | 99 ± 3% | 99 ± 5% | 99 ± 3% | 98 ± 5% |
| 12.50% | 91 ± 5% | 90 ± 6% | 89 ± 5% | 96 ± 3% | 98 ± 3% | 98 ± 3% | 98 ± 3% | 99 ± 3% | 99 ± 3% |
| 6.30% | 79 ± 11% | 81 ± 11% | 78 ± 10% | 94 ± 5% | 93 ± 5% | 94 ± 8% | 89 ± 8% | 89 ± 9% | 91 ± 9% |
| 3.10% | 41 ± 15% | 44 ± 15% | 43 ± 14% | 68 ± 16% | 74 ± 14% | 69 ± 17% | 80 ± 21% | 76 ± 22% | 75 ± 21% |
| AUC | | | | | | | | | |
| | Full sampling | | | 2-SpSCT | | | 4-SpSCT | | |
| Dose level | Central | seg. | sub-seg. | Central | seg. | sub-seg. | Central | seg. | sub-seg. |
| 100% | 0.96 ± 0.04% | 0.99 ± 0.03% | 0.99 ± 0.03% | \ | \ | \ | \ | \ | \ |
| 50% | 0.97 ± 0.06% | 1.00 ± 0.0% | 1.00 ± 0.0 | 0.98 ± 0.04% | 0.98 ± 0.05% | 0.97 ± 0.06% | \ | \ | \ |
| 25% | 0.99 ± 0.02% | 0.99 ± 0.03% | 0.98 ± 0.03% | 1.00 ± 0.0% | 1.00 ± 0.0% | 1.00 ± 0.0% | 0.98 ± 0.02% | 1.00 ± 0.0% | 1.00 ± 0.0% |
| 12.50% | 0.99 ± 0.01% | 0.99 ± 0.02% | 0.98 ± 0.04% | 0.99 ± 0.02% | 1.00 ± 0.0% | 1.00 ± 0.0% | 0.98 ± 0.02% | 0.98 ± 0.04% | 1.00 ± 0.0% |
| 6.30% | 0.94 ± 0.06% | 0.96 ± 0.03% | 0.92 ± 0.05% | 0.99 ± 0.02% | 0.97 ± 0.04% | 0.97 ± 0.05% | 0.97 ± 0.04% | 0.97 ± 0.04% | 1.00 ± 0.01% |
| 3.10% | 0.69 ± 0.18% | 0.76 ± 0.10% | 0.71 ± 0.05% | 0.89 ± 0.10% | 0.96 ± 0.02% | 0.88 ± 0.07% | 1.00 ± 0.01% | 0.96 ± 0.04% | 0.95 ± 0.04% |
| Interreader agreement (detection of PE) | | | | | | | | | |
| | Full sampling | | | 2-SpSCT | | | 4-SpSCT | | |
| Dose level | Central | seg. | sub-seg. | Central | seg. | sub-seg. | Central | seg. | sub-seg. |
| 100% | 0.784 | 0.791 | 0.589 | \ | \ | \ | \ | \ | \ |
| 50% | 0.73 | 0.751 | 0.422 | 0.831 | 0.853 | 0.619 | \ | \ | \ |
| 25% | 0.58 | 0.618 | 0.224 | 0.738 | 0.876 | 0.534 | 0.722 | 0.817 | 0.517 |
| 12.50% | 0.58 | 0.414 | 0.186 | 0.621 | 0.689 | 0.321 | 0.599 | 0.691 | 0.481 |
| 6.30% | 0.309 | 0.28 | 0.194 | 0.39 | 0.545 | 0.222 | 0.562 | 0.626 | 0.312 |
| 3.10% | 0.154 | 0.175 | 0.053 | 0.32 | 0.284 | 0.077 | 0.334 | 0.267 | 0.139 |

**Table 3** Confidence for the diagnosis of PE. Numbers are the average count of cases rated with high confidence (1, 2 or 5, 6), given as arithmetic mean ± SD. Total number of cases is 20

| Cases rated with high confidence (1, 2 or 5, 6) | | | | | | | | | |
|---|---|---|---|---|---|---|---|---|---|
| | Full sampling | | | 2-SpSCT | | | 4-SpSCT | | |
| Dose level | Central | seg. | sub-seg. | Central | seg. | sub-seg. | Central | seg. | sub-seg. |
| 100% | 19.8 ± 0.5 | 19.8 ± 0.5 | 19.5 ± 0.6 | \ | \ | \ | \ | \ | \ |
| 50% | 19.8 ± 0.5 | 19.8 ± 0.5 | 18.5 ± 1.0 | 20.0 ± 0.0 | 20.0 ± 0.0 | 19.5 ± 1.0 | \ | \ | \ |
| 25% | 19.5 ± 0.6 | 19.5 ± 0.6 | 18.3 ± 2.2 | 19.8 ± 0.5 | 19.8 ± 0.5 | 19.3 ± 1.0 | 19.8 ± 0.5 | 19.5 ± 1.0 | 19.3 ± 1.5 |
| 12.5% | 18.3 ± 1.0 | 18.5 ± 1.0 | 16.0 ± 2.9 | 19.5 ± 0.6 | 19.8 ± 0.5 | 18.3 ± 1.0 | 20.0 ± 0.0 | 20.0 ± 0.0 | 18.8 ± 1.9 |
| 6.3% | 15.8 ± 1.7 | 16.0 ± 2.4 | 12.3 ± 4.0 | 18.3 ± 1.3 | 18.8 ± 1.0 | 17.5 ± 1.7 | 18.3 ± 1.7 | 17.8 ± 1.7 | 17.0 ± 2.0 |
| 3.1% | 9.8 ± 3.9 | 8.8 ± 3.4 | 6.8 ± 4.3 | 15.0 ± 2.9 | 14.3 ± 3.0 | 10.8 ± 2.1 | 15.8 ± 4.7 | 15.5 ± 4.2 | 13.0 ± 2.4 |

(7.5%) to 0 by applying 4-SpSCT instead of FS at the 12.5% dose level. At this dose level, sensitivities of 100%/97.5%/100% for central/segmental/subsegmental PE could be achieved with 4-SpSCT, compared with 91.7%/90%/90% for FS. The effect of a more considerable difference between FS and 4-SpSCT at lower dose levels was expected as the sparse sampling technique is especially effective at lower dose levels. This is due to an increased noise at lower tube currents, and with sparse sampling, higher tube currents can be used compared with FS at the same dose level.

Taking all results into account, 4-SpSCT is superior to FS at all dose levels with greater differences at lower dose levels. In consequence, a dose reduction of 87.5% based on the already relatively low used dose in our department seems possible using MLRI and SpSCT, resulting in a mean ED of 0.38 mSv while maintaining acceptable image quality without the necessity of a repetition of the examination due to bad image quality. This is especially important as a reduction of the mean radiation dose can be unraveled by repeated examinations.

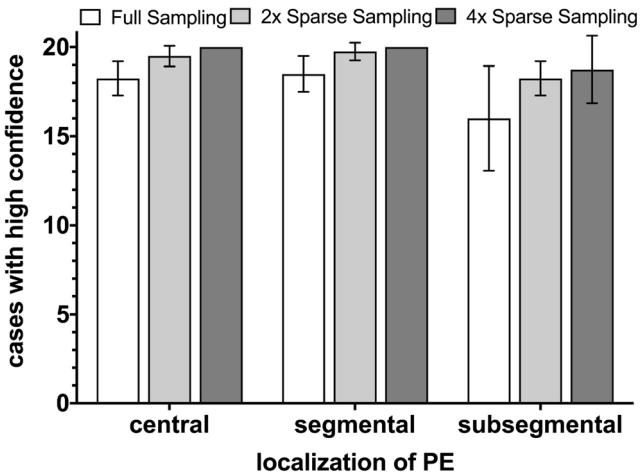


**Fig. 5** Average of cases rated with high confidence (1 or 2 and 5 or 6) at the 12.5% dose level for the different localizations of PE and sampling schemes

Regarding IQ, FS at 100% dose is superior to 4-SpSCT at the 25% dose level, which was the highest possible dose level to be simulated with 4-SpSCT. However, in clinical routine, 4-SpSCT could be performed with a lower dose reduction (e.g., 50%). Based on the results of the current study, these examinations should show higher IQ with less risk of performing a non-diagnostic exam while maintaining a significant dose reduction. At the lowest dose levels (6.3% and 3.1%, corresponding to 0.19 and 0.09 mSv, respectively), less examinations were rated as non-diagnostic and sensitivities were higher with 4-SpSCT compared with FS. However, according to the principle of "as low as reasonably achievable" (ALARA), a dose reduction to these values cannot be suggested even with comparatively good diagnostic performance with 4-SpSCT.

The present study has some limitations. Firstly, sparse sampling could only be simulated. However, sparse sampling can be simulated with high accuracy and simulated low-dose images are a well-established tool for studies [24, 25]. Secondly, a relatively low number of patients (20) were included in this study. This was due to the high number of image sets which had to be evaluated. A greater number of patients should be examined with fewer image sets per patient focused on the most relevant dose levels (i.e., 25%, 12.5%, and 6.3% dose). However, for this feasibility study, the numbers of patients and image sets seem appropriate as a completely novel imaging concept should be evaluated and diagnostic performance at the different dose levels could not be foreseen. Thirdly, all images were reconstructed with the same slice thickness and noise level to guarantee comparability. As all reconstructions (FS, SpSCT, low-dose images) were performed with the same slice thickness, a possible influence of slice thickness on the noise level should be present throughout all datasets. It is reasonable to assume that manually tuning noise parameters for each type of dataset (dose level and sparsity) would rather improve than degrade results for low dose levels. Depending on the chosen SpSCT and dose level, the noise level must be optimized when such systems are established.

In conclusion, the present study is the first to systematically evaluate sparse sampling as a potential future ultra-low-dose CT solution for detection of PE. Based on the results of the present study which was performed based on simulated sparse sampling images, a significant dose reduction using SpSCT in combination with fully iterative reconstruction (MLIR) seems feasible. At this moment, a dose reduction of 87.5% (corresponding to a mean ED of 0.38 mSv) for CTPA scans could be achieved while maintaining high subjective image quality as well as excellent diagnostic performance with sensitivities of nearly 100%.

**Acknowledgments** We thank Armin Ott (M.Sc.) for assistance with statistical analysis.

**Funding** This study has received funding by the German Department of Education and Research (BMBF) under grant IMEDO (13GW0072C) and the German Research Foundation (DFG) within the Research Training Group GRK 2274.

## Compliance with ethical standards

**Guarantor** The scientific guarantor of this publication is Dr. Andreas P. Sauter.

**Conflict of interest** Rolf Bippus and Roland Proksa are employees of Philips GmbH.

The remaining authors of this manuscript declare no relationships with any companies, whose products or services may be related to the subject matter of the article.

**Statistics and biometry** No complex statistical methods were necessary for this paper.

**Informed consent** Written informed consent was waived by the Institutional Review Board.

**Ethical approval** Institutional Review Board approval was obtained.

**Methodology**
- Retrospective
- Diagnostic or prognostic study
- Performed at one institution

## References

1. Goldhaber S (2012) Deep venous thrombosis and pulmonary embolism, New York
2. Estrada YMRM, Oldham SA (2011) CTPA as the gold standard for the diagnosis of pulmonary embolism. Int J Comput Assist Radiol Surg 6:557–563
3. Coche E, Verschuren F, Keyeux A et al (2003) Diagnosis of acute pulmonary embolism in outpatients: comparison of thin-collimation multi–detector row spiral CT and planar ventilation-perfusion scintigraphy. Radiology 229:757–765
4. Co SJ, Mayo J, Liang T, Krzymyk K, Yousefi M, Nicolaou S (2013) Iterative reconstructed ultra high pitch CT pulmonary angiography with cardiac bowtie-shaped filter in the acute setting: effect on dose and image quality. Eur J Radiol 82:1571–1576
5. Ohana M, Labani A, Jeung MY, Ghannudi SE, Gaertner S, Roy C (2015) Iterative reconstruction in single source dual-energy CT pulmonary angiography: is it sufficient to achieve a radiation dose as low as state-of-the-art single-energy CTPA? Eur J Radiol 84:2314–2320
6. Brenner DJ, Hall EJ (2007) Computed tomography–an increasing source of radiation exposure. N Engl J Med 357:2277–2284
7. Fingerle AA, Noel PB (2018) Dose reduction in abdominal CT: the road to submillisievert imaging. Eur Radiol. https://doi.org/10.1007/s00330-018-5397-z
8. Huda W, Atherton JV, Ware DE, Cumming WA (1997) An approach for the estimation of effective radiation dose at CT in pediatric patients. Radiology 203:417–422
9. Kalra MK, Rizzo S, Maher MM et al (2005) Chest CT performed with z-axis modulation: scanning protocol and radiation dose. Radiology 237:303–308
10. Willemink MJ, Noel PB (2018) The evolution of image reconstruction for CT-from filtered back projection to artificial intelligence. Eur Radiol. https://doi.org/10.1007/s00330-018-5810-7
11. Noel PB, Renger B, Fiebich M et al (2013) Does iterative reconstruction lower CT radiation dose: evaluation of 15,000 examinations. PLoS One 8:e81141
12. Sauter A, Koehler T, Fingerle AA et al (2016) Ultra low dose CT pulmonary angiography with iterative reconstruction. PLoS One 11:e0162716
13. Zizka J, Ryska P, Stepanovska J et al (2014) Iterative reconstruction of pulmonary MDCT angiography: effects on image quality, effective dose and estimated organ dose to the breast. Biomed Pap Med Fac Univ Palacky Olomouc Czech Repub 158:259–264
14. Sauter A, Koehler T, Brendel B et al (2018) CT pulmonary angiography: dose reduction via a next generation iterative reconstruction algorithm. Acta Radiol 0:284185118784976
15. Candes EJ, Romberg J, Tao T (2006) Robust uncertainty principles: exact signal reconstruction from highly incomplete frequency information. IEEE Trans Inf Theory 52:489–509
16. Donoho DL (2006) Compressed sensing. IEEE Trans Inf Theory 52:1289–1306
17. Koesters T, Knoll F, Sodickson A, Sodickson DK, Otazo R (2017) SparseCT: interrupted-beam acquisition and sparse reconstruction for radiation dose reduction SPIE Medical Imaging. SPIE, pp 7
18. Wiedmann U, Neculaes VB, Harrison D, Asma E, Kinahan PE, De Man B (2014) X-ray pulsing methods for reduced-dose computed tomography in PET/CT attenuation correction Medical Imaging 2014: Physics of Medical Imaging. International Society for Optics and Photonics, pp 90332Z
19. Kopp FK, Bippus R, Sauter AP et al (2018) Diagnostic value of sparse sampling computed tomography for radiation dose reduction: initial results SPIE Medical Imaging. SPIE, pp 6
20. Mei K, Kopp FK, Bippus R et al (2017) Is multidetector CT-based bone mineral density and quantitative bone microstructure assessment at the spine still feasible using ultra-low tube current and sparse sampling? Eur Radiol 27:5261–5271
21. Chen B, Muckley M, Sodickson A et al (2018) Evaluation of SparseCT on patient data using realistic undersampling models SPIE Medical Imaging. SPIE, pp 6
22. Zhao Z, Gang GJ, Siewerdsen JH (2014) Noise, sampling, and the number of projections in cone-beam CT with a flat-panel detector. Med Phys 41:061909
23. Huda W, Ogden KM, Khorasani MR (2008) Converting dose-length product to effective dose at CT. Radiology 248:995–1003
24. Muenzel D, Koehler T, Brown K et al (2014) Validation of a low dose simulation technique for computed tomography images. PLoS One 9:e107843

25. Zabic S, Wang Q, Morton T, Brown KM (2013) A low dose simulation tool for CT systems with energy integrating detectors. Med Phys 40:031102
26. Erdogan H, Fessler JA (1999) Ordered subsets algorithms for transmission tomography. Phys Med Biol 44:2835
27. Brown KM (2013) Sparse sampling for CT dose reduction. Proceedings of the Fully 3D 2013 Conference, pp 428–431
28. Bergner F (2012) Robust automated regularization factor selection for statistical reconstructions. Proceedings of the 2nd CT Meeting pp 267–270
29. Noël PB, Köhler T, Fingerle AA et al (2014) Evaluation of an iterative model–based reconstruction algorithm for low-tube-voltage (80 kVp) computed tomography angiography. J Med Imaging (Bellingham) 1:033501
30. Landis JR, Koch GG (1977) The measurement of observer agreement for categorical data. Biometrics 33:159–174
31. Hanley JA, McNeil BJ (1982) The meaning and use of the area under a receiver operating characteristic (ROC) curve. Radiology 143:29–36
32. Moser JB, Sheard SL, Edyvean S, Vlahos I (2017) Radiation dose-reduction strategies in thoracic CT. Clin Radiol 72:407–420
33. Muenzel D, Daerr H, Proksa R et al (2017) Simultaneous dual-contrast multi-phase liver imaging using spectral photon-counting computed tomography: a proof-of-concept study. Eur Radiol Exp 1: 25